

# Modelling of Reactive Spray Drying of Precursors for High $T_c$ Superconducting Ceramics

D. Depla, R. Mouton & S. Hoste

Laboratory for General and Inorganic Chemistry, University of Ghent, Krijgslaan 281, 9000 Ghent, Belgium

(Received 15 September 1995; revised version received 12 July 1996; accepted 15 July 1996)

## Abstract

One of the most efficient techniques used in the preparation of high quality precursor powder for the synthesis of high temperature superconducting ceramics (HTSC) involves spray drying of a solution of metal nitrates. This study describes our experiments in which particle size, shape and particle size distribution of the resulting products were examined by means of optical microscopy and SEM. To understand the formation of the powder a semi-empirical model which simulates the formation of the droplets and describes their drying path, was developed. © 1996 Elsevier Science Limited.

## Notation

$a$  Reaction coefficient  
 $A$  Chemical compound  
 $b$  Reaction coefficient  
 $B$  Chemical compound  
 $c$  Concentration  
 $C$  Constant  
ratio between inner and outer particle diameter  
 $D, d$  Diameter  
 $F$  Fraction of water remaining  
 $g$  Gravitation constant  
 $h$  Height  
Heat transfer coefficient  
 $H$  Humidity  
 $L$  Volume flow rate  
 $M$  Mass flow rate  
 $MM$  Molecule mass  
 $Q$  Heat  
 $S$  Solubility  
 $T$  Temperature  
 $V$  Velocity

$v$  Axial or radial component of velocity  
 $W$  Liquid mass flow rate  
 $x$  Co-ordinate  
 $y$  Co-ordinate

## Greek symbols

$\nabla$  Nabla operator  
 $\alpha$  Shape factor  
 $\delta$  Dispersion coefficient  
 $\phi$  Droplet size distribution  
 $\Gamma$  Gamma function  
 $\mu$  Viscosity  
 $\pi$  Constant (3.1415...)  
 $\rho$  Density  
correlation coefficient  
 $\sigma$  Surface tension  
Standard deviation

## Super- and subscripts

$A$  For chemical compound A  
 $B$  For chemical compound B or for area B  
 $cr$  Critical  
 $D$  With D: of the particle  
With C: drag coefficient  
 $dr$  Of the droplet  
With d: of the nozzle  
 $F$  Final  
 $g$  Of the gas  
 $h$  Axial  
 $i$  For first part  
 $l$  Of the liquid  
 $m$  With C: spreading coefficient  
 $o$  Initial  
 $r$  Radial  
 $rel$  Relative  
 $s$  Of the solid  
 $sur$  Of the surface  
 $vs$  Volume to surface or Sauter diameter  
 $x$  Of co-ordinate  $x$   
 $y$  Of co-ordinate  $y$

## 1 Introduction

From their synthesis point of view, high  $T_c$  superconducting ceramics (HTSC) are mixed oxides with special physical characteristics and whose preparation in bulk quantities involves the reaction of a mixture of metal oxides at elevated temperatures.<sup>1</sup> The reaction rate for their synthesis and the electrical, magnetic and mechanical qualities of the resulting HTSC are strongly influenced by the characteristics of the starting precursor mixture (homogeneity, particle size, chemical identity and composition,...). The easiest way to produce this precursor is through mechanical mixing of the different metal oxides. This simple process has been widely used in the ceramic industry.<sup>2</sup> Often however, the low homogeneity and purity of the powder results in a superconductor with poor physical and mechanical properties. To improve the properties of the HTSC several techniques, based on the conservation of the homogeneity of a precursor solution of metal salts, have been developed (coprecipitation,<sup>3</sup> sol-gel,<sup>4</sup> spray drying,<sup>5</sup> freeze drying,<sup>6</sup> hydrothermal synthesis<sup>6</sup>). One of the aims of these techniques is to produce a very homogeneous oxide mixture with small particle size and narrow particle size distribution. Although most of these techniques succeed in reproducibly producing a precursor with a fixed chemical composition and definite powder characteristics like particle size, shape and distribution, they lack flexibility when the ability to change the chemical composition or powder characteristics and a high throughput of material are required. Therefore spray drying holds much potential in the area of research on new superconducting materials. As shown in literature<sup>7</sup> and in contrast to most other techniques, the low complexity of spray drying makes modelling possible thus allowing the prediction of some powder characteristics. This approach reduces the number of preliminary experiments and accelerates the optimization of the process.

We have been using spray drying of nitrate solutions for the production of high quality  $\text{YBaCuO}_{7-\delta}$ ,<sup>8</sup>  $\text{BiPbSrCaCuO}_x$ <sup>9</sup> (2212 and 2223) superconductors using several spraying techniques encompassing high pressure capillary nozzles, two fluid concentric nozzles with co-current drying and piezo-electric mist production in a reactive spray drying configuration employing decomposition of the mist at elevated temperature (423–523 K). This study deals with the analysis of the powder characteristics obtained by a two-fluid co-current nebulizer used in conjunction with a modified, commercial spray drying apparatus.

To compare the predictions of the granulometry with the actual powder characteristics, one needs a good definition of the particle size and shape.

**Table 1.** Typical spray drying conditions for superconductor precursor

Inlet temperature	473-15 K
Outlet temperature	363-15-373-15 K
Air flow rate	750 Nl/h
Liquid flow rate	5 ml/min
Furnace temperature	973-15 K
Drying air flow rate	30 m <sup>3</sup> /h
Solution concentration	0.05 M for $\text{Y}(\text{NO}_3)_3 \cdot 6\text{H}_2\text{O}$

Therefore one must choose a particle size analysis (PSA) technique which takes the characteristics of the process into account. In the case of spray drying, this means that individual particles must be measured.

In this report we show that the combination of a correct PSA technique and a semi-empirical model allows a good description of the spray drying process. Based on some approximations, to be discussed, one can predict particle size and distribution with reasonable accuracy.

## 2 Experimental

Stoichiometric quantities of  $\text{Cu}(\text{NO}_3)_2 \cdot 3\text{H}_2\text{O}$ ,  $\text{Ba}(\text{NO}_3)_2$  and  $\text{Y}(\text{NO}_3)_3 \cdot 6\text{H}_2\text{O}$  were dissolved in distilled water to form an aqueous nitrate solution. Spray drying was performed using a modified Buchi spray dryer equipped with additional thermal insulation, an additional dryer furnace, exhaust cooler and gas scrubber (see Fig. 3). Typical spray drying conditions are given in Table 1. Nebulizing and drying was achieved using a two-fluid pneumatic nozzle in co-current configuration. Approximately 60 weight % of the original material can be recovered as a fine blue-grey powder in the cyclone collector.

Solution density was measured using a Paar Precision Density Meter, viscosity measurements were performed using Höppler Viscosity Meter. Surface tension was measured using the ring method. In order to measure the particle size, a small amount of the spray dried powder collected was suspended in canada balsam. Spots of this mixture were deposited on an object glass and were examined with an optical transmission microscope. The micrographs are scanned and analyzed using ImageView<sup>TM</sup> software. For SEM, a Phillips 501 scanning electron microscope was used.

## 3 Results

### 3.1 Particle size analysis

Each particle is regarded as a two-dimensional distribution of points (see Fig. 1) characterized by the ellipse of concentration.<sup>10</sup>

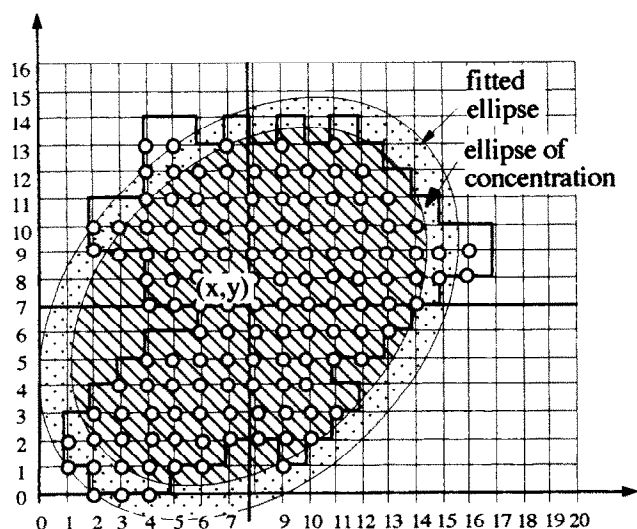


Fig. 1. Particle as two-dimensional distribution.

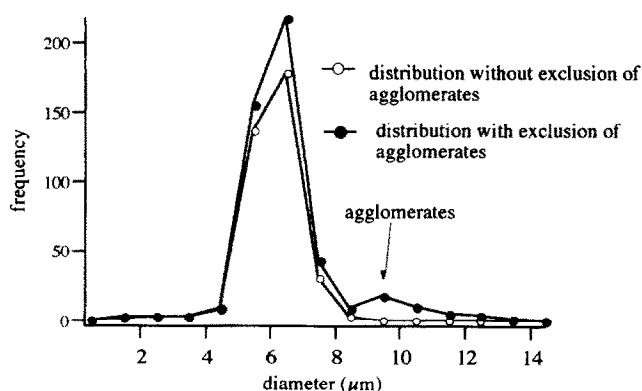


Fig. 2. Exclusion of agglomerates using the shape factor.

$$\frac{1}{1-\rho^2} \left( \frac{(x-\bar{x})^2}{\sigma_x^2} - \frac{2\rho(x-\bar{x})(y-\bar{y})}{\sigma_x\sigma_y} + \frac{(y-\bar{y})^2}{\sigma_y^2} \right) = 4 \quad (1)$$

where  $x$  and  $y$  are co-ordinates and  $\rho$  the correlation coefficient. The second-order central moments of the ellipse are equal to those of the distribution. After equalization of the surface of particle and

fitted ellipse, the particle size is defined as the arithmetical mean of the major and minor axes of the ellipse. A shape factor is calculated as follows:

$$\alpha = \frac{\text{minor axis}}{\text{major axis}} \cdot \frac{\text{perimeter of ellipse}}{\text{perimeter of particle}} \quad (2)$$

It can be shown mathematically that this shape factor is independent of the particle size. This shape factor can be used to separate the primary particles from the agglomerates. The combination of several primary particles creates a 'particle' whose perimeter is much larger than the one of the fitted ellipse and has a greater probability to be elongated. The combination of those two effects drastically reduces the shape factor. In order to study only the primary particles of a spray dried sample, all particles with a shape factor below the 25th percentile of the shape factor distribution were excluded (see Fig. 2). The particle size analysis used here was calibrated using diamond grinding powders and HPLC silica powders of known particle size.

### 3.2 Mathematical modelling

The spray drying process can be subdivided into four separate stages: (i) the transformation of the liquid into a spray, (ii) the mixing between the spray and the drying air, (iii) the drying of the droplets and (iv) the separation between the dried particles and the wet air.<sup>7</sup> As this separation process occurs mechanically in a cyclone and is not believed to influence formation of the particles, only the first three phenomena have been modelled as follows:

#### 3.2.1 Transformation of the liquid into a spray

For the calculation of the droplet size distribution (DSD) we used the two equations proposed by

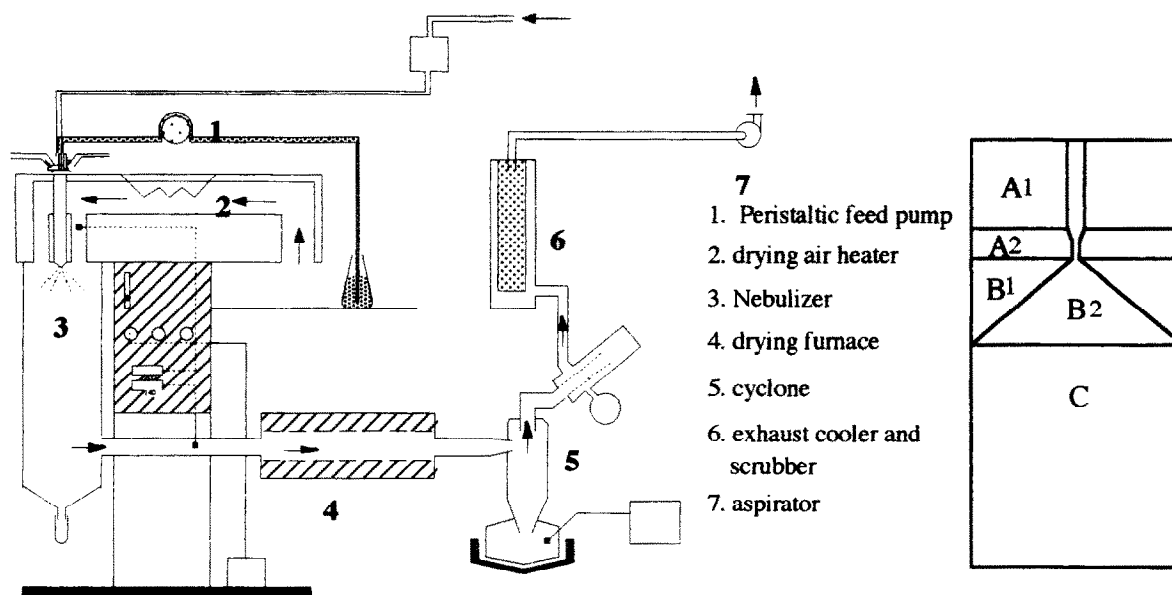


Fig. 3. Formal subdivision of the drying chamber and the modified Büchi spray dryer.

Nukiyama and Tanasawa for small capacity pneumatic nebulizers.<sup>11</sup>

$$D_{vs} = \frac{C_1}{V_{rel}} \left( \frac{\sigma_1}{\rho_1} \right)^{0.5} + C_2 \left( \frac{\mu_1}{\sqrt{\sigma_1 \rho_1}} \right)^{0.45} \left( \frac{\rho_1 L_1}{\rho_g L_g} \right)^{1.5} \quad (3)$$

$$\phi(D_{dr}) = \frac{\delta(5/\delta)^\delta D_{dr}^2}{D_{vs}^3 \Gamma(\delta/\delta)} \exp \left[ -(5/\delta)(D_{dr}/D_{vs})^\delta \right] \quad (4)$$

This first equation gives the Sauter diameter of the DSD as a function of the liquid characteristics, the ratio between liquid and mass flow rate and the relative velocity between nebulizing air and liquid. The second equation gives the DSD as a function of the Sauter diameter and the dispersion coefficient  $\delta$ . This coefficient is independent of the liquid characteristics and depends only on the nozzle itself. The Sauter diameter is defined as:

$$D_{vs} = \frac{\sum_{i=1}^n d_i^3}{\sum_{i=1}^n d_i^2} \quad (4')$$

### 3.2.2 Mixing between the spray and the drying air

The drying chamber of the spray dryer was conceptually divided into five areas (see Fig. 3). There is no mixing between the drying and nebulizing air in the A areas. The mixing starts to occur in the B area. As the nebulizing air expands (B2), the surrounding air (B1) is entrained. By using the equations of Baron and Alexander,<sup>12</sup> one can calculate the entrainment rate. The mass flow through a horizontal section of the cone can be written as follows:

$$M_{B1} = \pi \sqrt{\rho_g \rho_{g,o}} v_{g,h,o} d_e C_m h \quad (5)$$

Using the law of conservation of mass through the drying chamber, one can calculate the cone angle by iteration. In area C the mixing is complete and the droplets continue their path to the furnace and subsequently to the separating cyclone and filter bags.

### 3.2.3 Drying of the droplets

The equations describing the motion of the particles through the spray dryer are based on the results of Coulson and Richardson.<sup>13</sup>

$$\frac{dv_h}{dh} = -C_D \frac{3\rho_g}{4\rho_D D} \sqrt{(v_h - v_{gh})^2 + (v_r - v_{gr})^2} \left( \frac{v_h - v_{gh}}{v_h} \right) + \frac{g}{v_h} \left( 1 - \frac{\rho_g}{\rho_D} \right) \quad (6)$$

$$\frac{dv_r}{dh} = -C_D \frac{3\rho_g}{4\rho_D D} \sqrt{(v_h - v_{gh})^2 + (v_r - v_{gr})^2} \left( \frac{v_r - v_{gr}}{v_h} \right) \quad (7)$$

Table 2. Spray drying conditions of stearic acid

Flow rate nebulizing air	750 Nl/h
Air temperature	293.65 K
Average flow rate liquid stearic acid	4.20 ml/min
Average temperature of stearic acid	363.15 K

The velocity of the fluid is described by the equations of Baron and Alexander<sup>12</sup> for a free jet:

$$\overline{\nabla \cdot \rho_g v_{gh} V_g} = 0 \quad (8)$$

The heat transfer from the drying air to a particle is described by:

$$\frac{dQ}{dh} = h_c \frac{\pi D^2 (T_g - T_{sur})}{v_h} \quad (9)$$

An analogous equation can be written for the mass transfer from the particle to the surrounding air. The droplet temperature is assumed to be the wet bulb temperature.

The overall mass balance is written as follows:

$$\frac{F_i W_s + M_{B1,i} H_{B1,i} + [M_{B2,i} - M_{B2,ii}] M_{B2,o}}{F_{ii} W_s + M_{B1,ii} H_{B1,ii}} = \quad (10)$$

A similar equation can be written for the overall heat balance.

Based on these equations it is possible to calculate  $F$ , the fraction of water remaining, for each diameter class of the DSD. It is also possible to calculate the velocity, the change of the droplet temperature and density and the characteristics of the drying air (humidity, temperature). The influence of some spray drying parameters (initial temperature of drying air, flow rate of liquid and nebulizing air) on the overall fraction of water remaining can be simulated. The implementation of this model was written in Fortran-77.

## 4 Discussion

The dispersion coefficient, used to calculate the DSD in eqn (4) was determined from the measurements of the size of the droplets generated by the nozzle. The technical problems related to such a measurement can be solved by spray drying stearic acid which melts at 343.15 K and immediately solidifies when sprayed. Spray drying conditions are given in Table 2. To exclude possible effects of the cyclone, the spray dried particles were collected in a large vessel. After PSA, using above mentioned technique, eqn (4) was fitted to the experimental particle size distribution (PSD), resulting in the acceptable value<sup>7</sup> for  $\delta$  of 0.6648 (see Fig. 4).

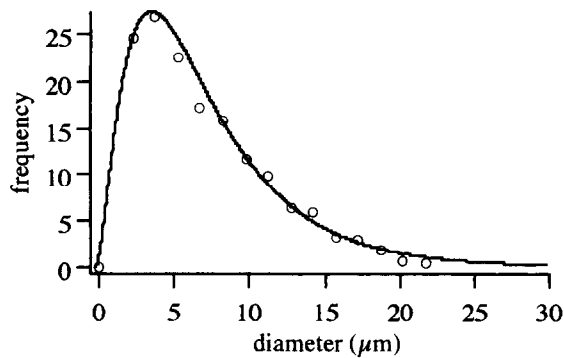
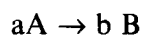


Fig. 4. Fitting of Nukiyama-Tanasawa distribution to experimental PSD of spray dried stearic acid.

In the concentration range used here, the liquid characteristics of the solution are almost equal to those of water. Nevertheless, the true liquid characteristics (viscosity, density and surface tension) were measured and used to calculate the DSD of the spray dried solutions.

As further research has shown,<sup>14</sup> the evaporation of water, at elevated temperatures, results in chemical decomposition of the nitrates of Y and Cu with the formation of hydroxy nitrate compounds. The reactions occurring during this reactive spray dry process can formally be written as:



To transform the DSD, in a first approach, into a PSD we can use eqn (11) which is based on the conservation of mass within each solid particle:

$$D_P = \sqrt[3]{\frac{b}{a} \frac{c_A M M_B}{\rho_B}} D_{dr} \quad (11)$$

By comparison of the theoretical PSD with an experimental PSD of spray dried superconductor precursor (see Fig. 5) a shift is noticed: the experimental particle size is much larger than the predicted size.

However, a detailed SEM investigation showed that the spray dried particles consisted of hollow

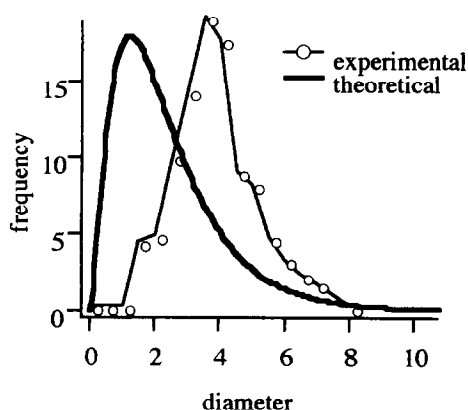


Fig. 5. Theoretical and experimental PSD for a spray dried  $YBaCuO_{7-\Delta}$  precursor.



Fig. 6. SEM image of spray dried particle (magnification: 11,000 x).

spheres (see Fig. 6). To take this effect into account we introduced the variable  $C$ , which is the ratio between the inner diameter and the outer particle diameter. After complete drying, eqn (11) can be transformed as follows, using the final value of  $C$ :

$$D_P = \sqrt[3]{\frac{c_o M M_s}{(1-C_F^3) \rho_s}} D_{dr} \text{ with } C_F = \left( \frac{D_{in}}{D_P} \right)_F \quad (12)$$

Based on the shift between the experimental and theoretical distribution (see Fig. 5),  $C_F$  or the crust thickness, can be calculated. In the case of the spray dried precursor (see Fig. 5) we calculated that the crust thickness is in the order of 0.1–0.2  $\mu\text{m}$ .

Experimental results of Charlesworth<sup>15</sup> and Parti<sup>16</sup> indicate that the drying process can be further subdivided in two stages. In an initial stage the evaporation of water results in a decrease of the droplet diameter. At a later stage, the droplet diameter stays constant as the solid crust becomes thicker. At a certain value of  $C$ ,  $C_{cr}$ , a transition from the first to the second stage occurs.  $C_{cr}$  can be deduced from the experimental value  $C_F$ :

$$\sqrt[3]{\frac{c_o M M_s S_s \rho_s (\rho_s - \rho_l)}{(\rho_{D,b} - \rho_l) \rho_s^2} \frac{\rho_l S_{s+}}{\rho_s} \frac{(\rho_s + \rho_l S_s) C_F^3}{\rho_s}} = C_{cr} \quad (13)$$

For non-reacting materials, no further approximations have to be made. In the presence of a chemical reaction, eqn (13) can only be used if one assumes that the reaction occurs after the particle has been dried and the influence of the reaction on the particle diameter is small.

Using  $C_{cr}$  in the mathematical model, the whole spray dry process can be simulated. To evaluate quality of the simulation, we spray dried a reference solution of  $Ba(NO_3)_2$  under the conditions given in Table 3. After PSA, a value for  $C_{cr} = 0.99$  was obtained. Simulations show that the largest droplets produced by the nozzle employed here,

cannot be totally dried in the Buchi spray dryer (see Fig. 7). This is not only due to the fact more water has to be evaporated but also, as Fig. 8 shows, because the relative velocity of the largest droplets versus the surrounding air is too high and decreases too slowly for them to avoid hitting the wall of the drying chamber.

**Table 3.** Spray drying conditions for a  $\text{Ba}(\text{NO}_3)_2$  solution

Solution temperature	298.15 K
Nebulizing air temperature	298.15 K
Inlet temperature	478.15 K
Outlet temperature	372.15 K
Flow rate nebulizing air	700 NI/h
Flow rate liquid	5 ml/min
Solution concentration	0.05 M

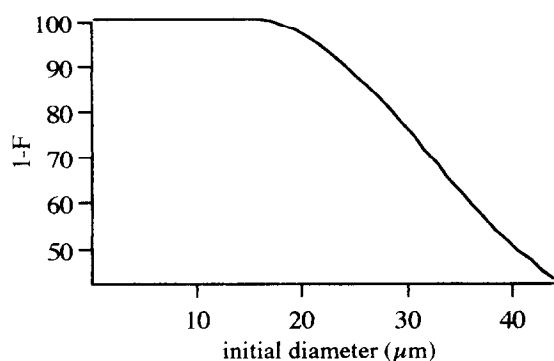


**Fig. 7.** Evaporated fraction as function of the initial class diameter of the DSD.

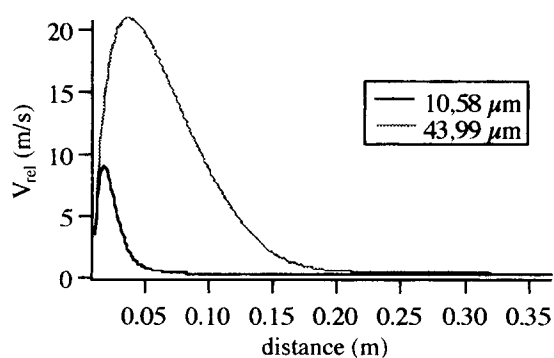


**Fig. 8.** Relative velocity of the droplets.

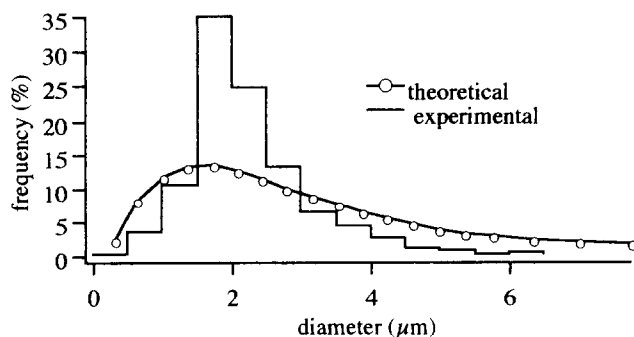


**Fig. 9.** Comparison between theoretical and experimental PSD on spray dried  $\text{Ba}(\text{NO}_3)_2$ .

If we exclude the diameter classes of those 'wet' particles (resulting water content  $> 5\%$ ) from the theoretical PSD, the comparison with the experimental one (see Fig. 9) yields a good agreement between the particle size ranges but a much narrower experimental PSD. This last observation can be attributed to the action of the cyclone.

Several other spray drying parameters were also simulated. In Figs 10–12 the effects of some parameters on the fraction of water remaining  $F$  are displayed. It is obvious that the use of hotter drying air reduces  $F$ . An increase of the flow rate of the nebulizing air reduces the average droplet size, while increasing the liquid flow rate has the opposite effect.

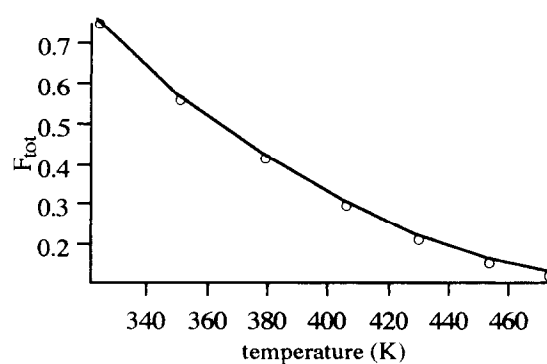


**Fig. 10.** Influence of the initial drying air temperature on  $F$ .

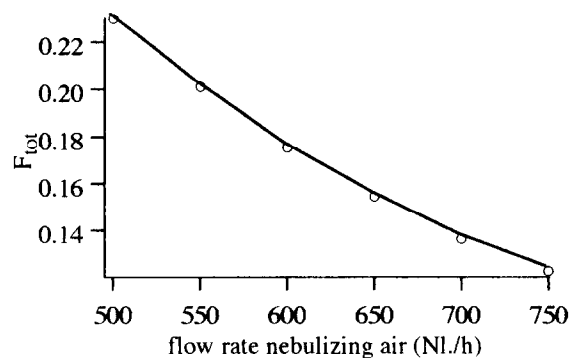


**Fig. 11.** Influence of the nebulizing airflow rate on  $F$ .

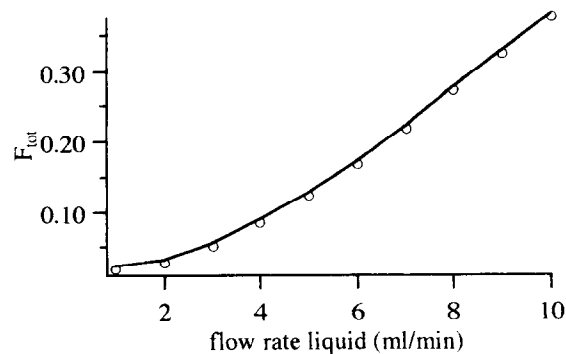


**Fig. 12.** Influence of the liquid flow rate on  $F$ .

## 5 Conclusion

Precursors for high  $T_c$  superconducting ceramics were spray dried from a nitrate solution. The particles obtained are hollow spheres with a average diameter of 4  $\mu\text{m}$  and possessing a thin crust. Our mathematical model explains the shape of the PSD and correctly predicts the characteristics of the drying air, the droplets and the resulting powder.

## Acknowledgement

This work has been supported by the Incentive Programme on High Temperature Superconductors supported by the Belgian State, Prime Minister's Service, Science Policy Office. Thanks are also due to the Vlaamse Instelling voor Technologisch Onderzoek, VITO, for some particle size analysis using optical diffraction. We gratefully acknowledge fruitful discussion with Prof. R. Verhoeven, University of Ghent.

## References

1. McGinn, P. In *High Temperature Superconducting Materials Science and Engineering*, ed. D. Shu. Pergamon, 1995, p. 345; Bourdillon, A. & Bourdillon, N. X. T., *High Temperature Superconductors, Processing and Science*, Academic Press, 1994, p. 93.
2. Kingery, W. D., Bowen, H. K. & Uhlmann, D. R., *Introduction to Ceramics*, 2nd edn. John Wiley, 1976.
3. Kaneko, K., Ihara, H., Hirabayashi, M., Terada, N. & Senzaki, K., *Jap. J. Appl. Phys.*, **26**, (1987) L734; Zhang, Yu, Fang, Z. H., Muhammed, M., Rao, K., Skumryev, V., Medelius, H. & Costa, J. L., *Physica C.*, **157** (1989) 108–114; Hsieh, P. Y., *Modern Physics Letters B.*, **4:6** (1990) 423; Vos, A., Mullens, J., Yperman, J., Carleer, R., Vanhees, J., Van Poucke, L. C., Krekels, T., Van Tendeloo, G., Persyn, F., Van Driessche, I. & Hoste, S. In *Superconductivity*, ed. B. Raveau *et al.* Technology Transfer Series, I.I.T.T.–ICMAS, Paris, 1991.
4. Kloucek, F., Rhine, W. E. & Bowen, H. K., *Physica C.*, **153–155** (1988) 798–799; Katayama, S. & Sekine, M., *J. Mat. Chem.*, **1:6** (1991) 1031; Nozue, A., Nasu, H., Kamiya, K. & Tanaka, K., *J. Mater. Sci.*, **26** (1991) 4427–4432; Hussain, A. A. & Sayer, M., *J. Appl. Physics*, **70** (1991) 1580.
5. Pebler, A., *Mat. Res. Bull.*, **24** (1988) 1069; Hsu, H. M., Yee, I., Deluca, J., Hilbert, C., Miracky, R. F. & Smith, L. N., *Appl. Phys. Lett.*, **54** (1989) 957; Blanchet, G., *Supercond. Sci. Technol.*, **4** (1991) 69; Sung, G. Y., Carter, C. B., Cho, D. H. & Kim, C. H., *J. Mater. Sci.*, **26** (1991) 1803; Tatsumisago, M., Tohge, M., Minami, T., Okuyama, K., Adochi, M., Kiada, Y. & Kaisoka, Y., *JJAP*, **30** (1991) 952.
6. Medelius, H. & Rowcliffe, D. J., *Mater. Sci. Eng.*, **4** (1989) 289.
7. Masters, K., *Spray Drying Handbook*. Longman Scientific and Technical, New York, 1991.
8. Hoste, S., Vlaeminck, H., DeRyck, P. H., Persyn, F., Mouton, R. & Van Der Kelen, G. P., *Supercond. Sci. Techn.*, **1** (1989) 239; Tanaka, M., Hoste, S., Suzuki, M., Isobe, M. & Ami, T., *Materials Letters*, **15** (1993) 334.
9. Van Driessche, I., Depla, D., Denul, J., De Roo, N., De Gryse, R. & Hoste, S., *Applied Superconductivity*, **2** (1994) 391.
10. Cramer, H., *Mathematical Methods of Statistics*. Princeton Univ. Press, NJ, 1945.
11. Dickinson, D. R. & Marshall, W. R. Jr, *AIChE Journal*, **14** (1968) 541.
12. Baron, T. & Alexander, L. C., *Chem. Eng. Prog.*, **47** (1951) 181.
13. Coulson, J. M. & Richardson, J. F., *Chemical Engineering*, Pergamon Press, 1991.
14. Depla, D. & Hoste, S., *Chromochimica Acta*, to be published.
15. Charlesworth, D. H. & Marshall, W. R. Jr, *AIChE Journal*, **6** (1960) 9.
16. Parti, M. & Paláncz, B., *Chem. Eng. Sci.*, **29** (1974) 355.